National Cancer Institute, 2003. http://ctep.cancer.gov/forms/CTCAEv3.pdf.
7. Altundag O, Gullu I, Altundag K *et al.* Induction chemotherapy with cisplatin and 5-fluorouracil followed by chemoradiotherapy or radiotherapy alone in the treatment of locoregionally advanced resectable cancers of the larynx and hypopharynx: results of single-center study of 45 patients. *Head Neck* 2005;**27**:15–21.
8. Lambert L, Fortin B, Soulieres D *et al.* Organ preservation with concurrent chemoradiation for advanced laryngeal cancer: are we succeeding? *Int J Radiat Oncol Biol Phys* 2010;**76**:398–402.
9. Fukada J, Shigematsu N, Takeda A *et al.* Weekly low-dose docetaxel-based chemoradiotherapy for locally advanced oropharyngeal or hypopharyngeal carcinoma: a retrospective, single-institution study. *Int J Radiat Oncol Biol Phys* 2010;**76**:417–24.
10. Mendenhall WM, Parsons JT, Stringer SP *et al.* Radiotherapy alone or combined with neck dissection for T1–T2 carcinoma of the pyriform sinus: an alternative to conservation surgery. *Int J Radiat Oncol Biol Phys* 1993;**27**:1017–27.
11. Nakamura K, Shioyama Y, Kawashima M *et al.* Multiinstitutional analysis of early squamous cell carcinoma of the hypopharynx treated with radical radiotherapy. *Int J Radiat Oncol Biol Phys* 2006;**65**:1045–50.
12. Vandenbrouck C, Eschwege F, De la Rochefordiere A *et al.* Squamous cell carcinoma of the pyriform sinus: retrospective study of 351 cases treated at the Institut Gustave-Roussy. *Head Neck Surg* 1987;**10**:4–13.
13. Chen SW, Yang SN, Liang JA *et al.* Prognostic impact of tumor volume in patients with stage III–IVA hypopharyngeal cancer without bulky lymph nodes treated with definitive concurrent chemoradiotherapy. *Head Neck* 2009;**31**:709–16.
14. Tai SK, Yang MH, Wang LW *et al.* Chemoradiotherapy laryngeal preservation for advanced hypopharyngeal cancer. *Jpn J Clin Oncol* 2008;**38**:521–7.
15. Mekhail TM, Adelstein DJ, Rybicki LA *et al.* Enteral nutrition during the treatment of head and neck carcinoma: is a percutaneous endoscopic gastrostomy tube preferable to a nasogastric tube? *Cancer* 2001;**91**:1785–90.
16. Fuwa N, Shibuya N, Hayashi N *et al.* Treatment results of alternating chemoradiotherapy for nasopharyngeal cancer using cisplatin and 5-fluorouracil – A phase II study. *Oral Oncology* 2007;**43**:948–55.
17. Kohmura T, Hasegawa Y, Matsuura H *et al.* Clinical analysis of multiple primary malignancies of the hypopharynx and esophagus. *Am J Otolaryngol* 2001;**22**:107–10.
18. Morimoto M, Nishiyama K, Nakamura S *et al.* Significance of endoscopic screening and endoscopic resection for esophageal cancer in patients with hypopharyngeal cancer. *Jpn J Clin Oncol* 2010;**40**:938–43.
19. Muto M, Minashi K, Yano T *et al.* Early detection of superficial squamous cell carcinoma in the head and neck region and esophagus by narrow band imaging: a multicenter randomized controlled trial. *J Clin Oncol* 2010;**28**:1566–72.

Journal of Radiation Research Advance Access published January 4, 2013

Journal of Radiation Research, 2013, pp 1–5
doi: 10.1093/jrr/rrs133

Phase I study of oral S-1 and concurrent radiotherapy in patients with head and neck cancer

Kensei NAKATA[1,*], Koh-ichi SAKATA[1], Masanori SOMEYA[1], Katsutoshi MIURA[1], Junichi HAYASHI[1], Masakazu HORI[1], Masaru TAKAGI[1], Tetsuo HIMI[2], Atsushi KONDO[2] and Masato HAREYAMA[1]

[1]Department of Radiology, Sapporo Medical University, S-1, W-16, Chuo-ku, Sapporo, 060-8543, Japan
[2]Department of Otolaryngology, Sapporo Medical University, S-1, W-16, Chuo-ku, Sapporo, 060-8543, Japan
*Corresponding author. Department of Radiology, Sapporo Medical University. S-1, W-16, Chuo-ku, Sapporo, 060-8543, Japan. Tel: + 81-11-611-2111 ext. 3535; Fax: + 81-11-613-9920; Email: kensei@sapmed.ac.jp

(Received 9 April 2012; revised 5 December 2012; accepted 5 December 2012)

This study investigated the maximum tolerated dose (MTD) of S-1 with concurrent radiotherapy in patients with head and neck cancer, based on the frequency of dose-limiting toxicities (DLT). S-1 was administered orally at escalating doses from 40 mg/m^2 b.i.d. on the days of delivering radiotherapy, which was given at a total dose of 64–70 Gy in 32–35 fractions over 6–7 weeks. A total of 12 patients (3 patients at 40 mg/m^2, 6 patients at 60 mg/m^2, and 3 patients at 80 mg/m^2) were enrolled in this trial. At the dose of 80 mg/m^2, two of the three patients developed DLT (Grade 3 anorexia and rhabdomyolysis) due to S-1, so the MTD was determined to be 80 mg/m^2. Among the 12 enrolled patients, 9 (75%) showed a complete response and 3 (25%) showed a partial response. The overall response rate was 100%. The recommended dose of S-1 with concurrent radiotherapy is 60 mg/m^2.

Keywords: head and neck cancer; chemoradiotherapy; S-1; Phase I study

INTRODUCTION

Platinum-based chemotherapy has been the chief regimen used in studies of concurrent chemoradiotherapy (CCRT) [1]. However, platinum-based regimens cannot be administered to patients with features such as advanced age, renal dysfunction, or refusal of hospitalization. Therefore, chemotherapy that can be delivered to such patients during radiotherapy is required.

S-1 is a novel oral drug, which is a combination of tegafur, 5-chloro-2,4-dihydroxypyridine (gimeracil), and potassium oxonate (oteracil) at a 1:0.4:1 molar concentration ratio [2]. Tegafur is hydroxylated and converted to 5-FU by hepatic microsomal enzymes. After intravenous injection, more than 85% of 5-FU is rapidly catabolized by the enzyme dihydropyrimidine dehydrogenase (DPD) [3]. Gimeracil is a competitive inhibitor of DPD that prevents the rapid degradation of 5-FU, and acts to maintain effective 5-FU levels in the plasma and tumor tissue. It is 180 times more potent than uracil, the DPD inhibitor found in uracil-tegafur (UFT), so an effective concentration of 5-FU is maintained in both the plasma and tumor tissue after S-1 administration [4]. We previously found that gimeracil also has a radiosensitizing effect by inhibiting the repair of double-stranded DNA breaks [5]. Oteracil is a competitive inhibitor of orotate phosphoribosyltransferase (OPRT), which inhibits phosphorylation of 5-FU in the gastrointestinal tract and thus reduces serious gastrointestinal toxicity associated with 5-FU therapy [6].

The antitumor effect of S-1 has already been demonstrated in patients with a variety of solid tumors, including advanced gastric cancer [7], colorectal cancer [8], non-small-cell lung cancer [9], and head and neck cancer [10]. Thus, S-1 has shown promising antitumor activity against head and neck cancer, and is much more convenient than continuous intravenous 5-FU infusion as it is administered orally. Radiotherapy could be combined with S-1 therapy in patients for whom platinum-based chemotherapy is not applicable. Therefore, we conducted a Phase I trial to determine the maximum tolerated dose of S-1 with concurrent radiotherapy in patients with head and neck cancer, based on the frequency of dose-limiting toxicities (DLT).

© The Author 2013. Published by Oxford University Press on behalf of The Japan Radiation Research Society and Japanese Society for Therapeutic Radiology and Oncology.
This is an Open Access article distributed under the terms of the Creative Commons Attribution Non-Commercial License (http://creativecommons.org/licenses/by-nc/3.0/), which permits unrestricted non-commercial use, distribution, and reproduction in any medium, provided the original work is properly cited.

MATERIALS AND METHODS

Eligibility

Patients with histopathologically proven squamous cell carcinoma of the head and neck were eligible for this study. They were required to be at least 20 years old, to have an Eastern Cooperative Oncology Group performance status of 2 or less, and to have adequate organ function (leukocytes ≥ 3500/mm^3, platelets ≥ 100 000/mm^3, hemoglobin ≥ 9.0 g/dl, normal serum creatinine and blood urea nitrogen, serum glutamic oxaloacetic transaminase (GOT) ≤ 100 U/l, serum glutaminic pyruvic transaminase (GPT) ≤ 100 U/l, and serum albumin ≥ 3.0 g/dl). Patients were excluded if they had received prior systemic therapy or radiotherapy, had another active malignancy, active infection, active gastric/duodenal ulcer, severe concurrent disease, or mental disorder.

This study was performed according to the guidelines of the Declaration of Helsinki (as amended in Edinburgh, Scotland in October 2000) and its protocol was approved by the Institutional Review Board of Sapporo Medical University School of Medicine. All patients gave written informed consent before being enrolled in this study.

Treatment

Fig. 1 shows the treatment schedule. Radiotherapy was initiated on Day 1 of the study using 4 MV photons. A fractional daily dose of 2.0 Gy (5 days/week) at the isocenter was given till a total dose of 64–70 Gy had been administered. Treatment planning was performed with a CT simulator (Asteion; Toshiba Medical Systems, Tokyo, Japan) for all patients, and the dose distribution was calculated with a 3D treatment planning system (Xio; CMS Japan KK, Tokyo, Japan).

S-1 (Taiho Pharmaceutical Co., Tokyo, Japan) was administered orally twice a day after meals every day, except on the weekends and holidays when radiotherapy was not performed. Each capsule of S-1 contained 20 or 25 mg of tegafur, and individual doses were rounded down to the nearest amount less than the dose calculated according to the body surface area, using the two available formulations.

The initial dose of S-1 was 40 mg/m^2/day (Level 1), and the dose was escalated to 60 mg/m^2/day (Level 2) and 80 mg/m^2/day (Level 3). The initial dose level of S-1 (40 mg/m^2/day) was selected because it was deemed to be safe based on our prior experience of S-1 (50 mg/body/day) chemoradiotherapy (CRT).

Evaluations during CRT included a weekly history, physical examination, hematology and biochemistry, and assessment of toxicity. DLT was defined as Grade 3 or 4 nonhematologic toxicity (excluding Grade 3 radiation mucositis and dermatitis), Grade 4 hematologic toxicity occurring during treatment or within two weeks after completing treatment, or requirement for suspension of either S-1 or radiation therapy for seven days or more. If mucositis became severe, we managed it with appropriate analgesics and mucosal protective agents in order to alleviate the symptoms. If none of the three patients experienced any DLTs at a given dose level, the dose of S-1 was escalated for the next cohort of three patients. If one of the initial three patients experienced a DLT, three more patients were added at that dose level. Dose escalation continued if DLTs were only observed in one or two out of six patients. If three or more patients experienced DLTs at a dose level, the previous dose level was defined as the maximum tolerated dose (MTD). Thus, if two or three of the initial three patients experienced DLTs, the starting dose level would be the MTD.

RESULT

Patient characteristics

A total of 12 patients were enrolled in this study between April 2008 and December 2009. The characteristics of the eligible patients are outlined in Table 1: Nine of the patients were men and three were women, with a median age of 71 years. None of the patients had received prior chemotherapy or radiation therapy.

Toxicity

All treated patients ($n = 12$) were assessed for toxicities. The toxicities observed during treatment or within two weeks of completing treatment are listed in Table 2. Three patients were treated with S-1 at dose Level 1 (40 mg/m^2/day) and six patients at dose Level 2 (60 mg/m^2/day). Of the latter, one experienced rapid-onset Grade 1 thrombocytopenia with a systemic maculopapular rash. After the

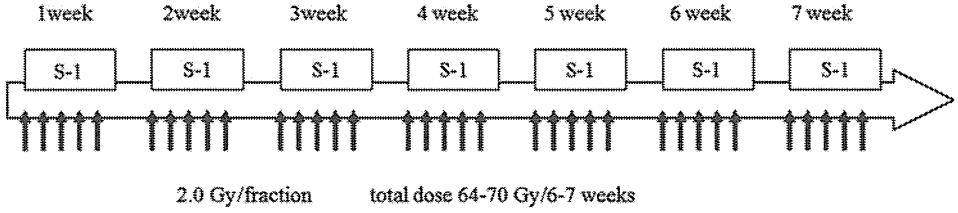

Fig. 1. The treatment schedule: S-1 was administered by the amount at each level on the day with the radiation therapy. Radiation therapy was delivered as a total dose of 64–70 Gy in 32–35 fractions over 6–7 weeks.

Table 1. Background of the patients

Case	Age	Sex	Tumor site	Classified TNM	S-1	RT	Eq. Sqm	Efficacy
Level 1								
1	59	M	Supra glottic	T1N0M0	40 (60)	70	9.2	CR
2	62	M	Supra glottic	T2N0M0	40 (60)	68	9.2	CR
3	55	F	Oropharynx	T2N1M0	40 (50)	70	10.5	CR
Level 2								
4*	79	M	Neck L/N	TxN3M0	60 (80)	70	10.0	PR
5	64	M	Glottic	T2N0M0	60 (90)	70	6.0	CR
6	70	M	Hypopharynx	T2N1M0	60 (80)	70	13.5	CR
7*	79	F	Buccal membrane	T1N0M0	60 (80)	66	8.3	CR
8	83	M	Supra glottic	T2N0M0	60 (80)	66	8.3	CR
9	76	M	Subglottic	T2N0M0	60 (90)	66	10.6	CR
Level 3								
10	72	F	External auditory canal	T4N0M0	80 (100)	64	7.7	PR
11*	69	M	Supra glottic	T2N0M0	80 (120)	70	9.2	PR
12*	77	M	Hypopharynx	T2N2bM0	80 (120)	66	16.0	CR

S-1 = dose of daily S-1 mg/m^2 (mg/body), RT = total radiation dose (Gy), Eq. Sqm = equivalent square meter of radiation field length (cm), * = patient who experienced dose-limiting toxicity.

dose of S-1 was reduced, there was no improvement of these symptoms, so S-1 was stopped. In addition, one patient experienced Grade 3 mucositis at a radiation dose of approximately 20 Gy.

Of the initial three patients treated with S-1 at dose Level 3 (80 mg/m^2/day), one experienced Grade 4 anorexia and one experienced an increase of serum CPK due to rhabdomyolysis caused by S-1.

After treatment was stopped, these adverse events all improved. There were no Grade 2 or higher events in any of the patients.

Response and survival

At the initial evaluation immediately after CRT, a complete response was seen in 9 (75%) of all 12 patients and a partial response was seen in 3 (25%). Stable disease or progressive disease was not encountered. During a median follow-up period of 35 months (range, 3–45 months), distant metastases developed in 1 patient and local failure occurred in 1 patient.

DISCUSSION

The main goal of this study was to find the dose of S-1 that could be safely combined with radiotherapy in patients with head and neck cancer. Radiation alone is the standard treatment for T1 or T2 glottic cancer and T1N0M0 nasopharyngeal cancer [11]. However, treatment with radiation alone does not achieve satisfactory results in patients with other head and neck tumors that are T1–2 and N0 [12]. Concurrent chemoradiotherapy might be one possibility for improving the outcomes for these patients [13], so we included head and neck cancer patients with T1–2N0M0 tumors other than cancer of the glottis or nasopharynx in this study.

Because severe mucositis is one of the major complications of radiotherapy for head and neck cancer, it is often difficult to determine whether CRT or RT has caused it, so Grade 3 mucositis was excluded from DLT assessment in this study. Instead, we defined DLT as suspension of treatment for more than 7 days, so that it included severe mucositis which prevented patients from taking S-1. We think that oral administration of S-1 is important, because its main benefit is that we can treat patients on an ambulatory basis.

In general, the intensity of the side effects depends on the size of the radiation field. In this study, the average equivalent square meter (Eq.Sqm) field length was 9.9 cm (range, 6.0–16.0 cm). At dose Level 3, the Eq.Sqm of the patient with a DLT was 16 cm. This patient developed Grade 3 mucositis that might have been due to a large radiation field. However, the reason for discontinuing S-1 was the increase of serum CPK. In patients with early head and neck cancer, the planning target volume is localized to the primary tumor, so the radiation field is smaller than for that of advanced head and neck cancer. If the average radiation

Table 2. Toxicities

	NCI-CTC Grade					≧Grade 3
	0	1	2	3	4	
Level 1: $n=3$ (S-1 40 mg/m^2)						
Leukopenia	2		1			
Hemoglobinpenia		3				
Thrombocytopenia	3					
Dermatitis		1	1	1		33%
Mucositis		1	2			
Dysphagia			3			
Diarrhea	3					
Level 2: $n=6$ (S-1 60 mg/m^2)						
Leukopenia	2	3	1			
Hemoglobinpenia	1	4	1			
Thrombocytopenia	4	2				
Dermatitis			1	5		83%
Mucositis	1	1	3	1		17%
Dysphagia		3	2	1		17%
Diarrhea	6					
Level 3: $n=3$ (S-1 80 mg/m^2)						
Leukopenia	1	2				
Hemoglobinpenia	1	2				
Thrombocytopenia	3					
Dermatitis			3			
Mucositis	1		1	1		33%
Dysphagia	2			1		33%
Diarrhea	2		1			

field was smaller than that used in this study, the MTD may be higher than our result. However, CRT is generally not indicated for early head and neck cancer, which is usually treated with small-field radiotherapy.

The rationale for CCRT is that chemotherapy agents may act as radiation sensitizers in addition to contributing their own antitumor effect [14]. In this study, we set up the administration schedule for S-1 expecting that gimeracil and 5-FU would act as sensitizers for radiotherapy. Therefore, we considered that the administration of S-1 on each day of radiotherapy was essential and we used the following schedule: S-1 was administered every day except on hospital holidays when radiotherapy was not delivered.

Chemoradiation schedules with S-1 that have previously been reported all included some weeks of planned S-1 suspension during radiotherapy. Tsuji *et al.* reported the results of an S-1 dose escalation study with 2 weeks of S-1 administration followed by 2 weeks off S-1, and then 2 more weeks of S-1 administration during radiotherapy (total dose: 60 Gy). They reported that the recommended dose (RD) of S-1 was 80 mg/body/day with their schedule [15]. Sato *et al.* reported that the RD of S-1 was 65 mg/m^2/day when radiation was given to a total dose of 60 Gy and S-1 was administered every day for 2 weeks and then was suspended for 1 week [16]. In addition, Tsukuda *et al.* reported that the RD of S-1 was 80–100 mg/body/day when radiation was given to a total dose of 60–70.2 Gy, and S-1 was administered every day for 2 weeks and was then suspended for 1 week [17]. Furthermore, Harada *et al.* reported the results of an S-1 dose escalation study that had almost the same schedule as our study. They stated that the RD of S-1 to be 65 mg/m^2/day with administration on 5 days per week [18]. The difference from our study is that their total radiation dose was only 40 Gy because they were giving preoperative concurrent chemoradiotherapy. There have been other reports on Phase III trials of radiotherapy with S-1 [19–23] or the combination of S-1 and cisplatin/nedaplatin [24–26] for head and neck cancer. These studies have demonstrated that S-1 and concurrent radical radiotherapy is safe and well tolerated by patients with complications and is a patient-friendly treatment. In the CRT schedules of all these studies, some weeks of planned interruption of S-1 administration occurred during radiation therapy. To the best of our knowledge, therefore, this is the first Phase I trial of concurrent S-1 and radical radiotherapy for head and neck cancer, in which S-1 was administered continuously during the period of radiotherapy.

In this study, oral S-1 and concurrent radiotherapy were well tolerated and feasible. The MTD was reached at dose Level 3 (80 mg/m^2/day), so we concluded that the RD of S-1 with concurrent radiotherapy is 60 mg/m^2/day. Compliance with the regimen was satisfactory and all patients completed their planned radiotherapy. Evaluation of efficacy was not the primary objective of this small Phase I study. To evaluate the long-term outcomes and potential late complications of our regimen, we will continue to accumulate patients and follow them over the long term. We are currently conducting a Phase II study of S-1 and concurrent radical radiotherapy in patients who are not suitable for platinum-based chemoradiotherapy.

CONCLUSION

In conclusion, this study showed that S-1 and concurrent radical radiotherapy is feasible and well tolerated in patients with head and neck cancer. The RD of S-1 with concurrent radiotherapy was determined to be 60 mg/m^2/body on every day of radiation delivery. This combination therapy may be an attractive alternative to conventional CRT using infused 5-FU for head and neck cancer because of its convenience and feasibility.

ACKNOWLEDGEMENTS

This article was presented at the ASTRO 52nd annual meeting held in October-November 2010.

FUNDING

This work was supported by Sapporo Medical University.

REFERENCES

1. Pignon JP, le Maître A, Maillard E *et al.* Meta-analysis of hemotherapy in head and neck cancer (MACH-NC): an update on 93 randomised trials and 17,346 patients. *Radiother Oncol* 2009;**92**:4–14.
2. Shirasaka T, Shimamoto Y, Ohshima H *et al.* Development of a novel form of an oral 5-fluorouracil derivative (S-1) directed to the potentiation of the tumor selective cytotoxicity of 5-fluorouracil by two biochemical modulators. *Anticancer Drugs* 1996;**7**:548–57.
3. Heggie GD, Sommandossi JP, Cross DS *et al.* Clinical pharmacokinetics of 5-fluorouracil and its metabolites in plasma, urine, and bile. *Cancer Res* 1987;**47**:2203–6.
4. Tatumi K, Fukushima M, Shirasaka T *et al.* Inhibitory effects of pyrimidine, barbituric acid and pyridine derivatives on 5-fluorouracil degradation in rat liver extracts. *Jpn J Cancer Res* 1987;**78**:748–55.
5. Takagi M, Sakata K, Someya M *et al.* Gimeracil sensitizes cells to radiation via inhibition of homologous recombination. *Radiother Oncol* 2010;**96**:259–66.
6. Shirasaka T, Shimamoto Y, Fukushima M. Inhibition by oxonic acid of gastrointestinal toxicity of 5-fluorouracil without loss of its antitumor activity in rats. *Cancer Res* 1993;**53**:4004–9.
7. Sakata Y, Ohtsu A, Horikoshi N *et al.* Late phase II study of novel oral fluoropyrimidine anticancer drug S-1 (1 M tegafur-0.4 M gimestat-1 M otastat potassium) in advanced gastric cancer patients. *Eur J Cancer* 1998;**34**:1715–20.
8. Ohtsu A, Baba H, Sakata Y *et al.* Phase II study of S-1, a novel oral fluorophyrimidine derivative, in patients with metastatic colorectal carcinoma. S-1 Cooperative Colorectal Carcinoma Study Group. *Br J Cancer* 2000;**83**:141–5.
9. Kawahara M, Furuse K, Segawa Y *et al.* Phase II study of S-1, a novel oral fluorouracil, in advanced non-small-cell lung cancer. *Br J Cancer* 2001;**85**:939–43.
10. Inuyama Y, Kida A, Tsukukda M *et al.* Late phase II study of S-1 in patients with advanced head and neck cancer. *Gan To Kagaku Ryoho* 2001;**28**:1381–90.
11. National Comprehensive Cancer Network Guidelines Head and Neck Cancers Version 1.2012. http://www.nccn.org/professionals/physician_gls/pdf/head-and-neck.pdf (10 September 2012, date last accessed).
12. Leonard L, Gunderson Joel E *et al. Clinical Radiation Oncology.* 2nd edn. Philadelphia, Pennsylvania: Churchill Livingstone, 2006, 639–754.
13. Goshi N, Mamoru T, Yasukazu M *et al.* Efficacy of concurrent chemoradiotherapy for T1 and T2 laryngeal squamous cell carcinoma regarding organ preservation. *Anticancer Res* 2009;**29**:661–6.
14. Douple EB, Richmond RC, O'Hara JA *et al.* Carboplatin as a potentiator of radiation therapy. *Cancer Treat Rev* 1985;**12** (Suppl A): 111–24.
15. Tsuji H, Nagata M, Inoue T *et al.* Clinical Phase I trial of concurrent chemo-radiotherapy with S-1 for T2N0 glottic carcinoma. *Jpn J Cancer Chemother* 2006;**33** Suppl 1:163–6.
16. Sato M, Harada K. Phase I study of concurrent radiotherapy with S-1 for oral squamous cell carcinoma. *Jpn J Cancer Chemother* 2006;**33** (Suppl 1):179–83.
17. Tsukuda M, Ishitoya J, Mikami Y *et al.* Analysis of feasibility and toxicity of concurrent chemoradiotherapy with S-1 for locally advanced squamous cell carcinoma of the head and neck in elderly cases and/or cases with comorbidity. *Cancer Chemo Pharm* 2009;**64**:945–52.
18. Harada H, Omura K. Preoperative concurrent chemotherapy with S-1 and radiotherapy for locally advanced squamous cell carcinoma of the oral cavity: phase I trial. *J Exp Clin Cancer Res* 2010;**29**:33.
19. Nakashima T, Toh S, Shiratsuchi H *et al.* Laryngeal preservation for hypopharyngeal cancer by radiotherapy with S-1 and vitamin A (TAR therapy). *Gan To Kagaku Ryoho* 2012;**39**:759–63.
20. Ohnishi K, Shioyama Y, Nakamura K *et al.* Concurrent chemoradiotherapy with S-1 as first-line treatment for patients with oropharyngeal cancer. *J Radiat Res* 2011;**52**:47–53.
21. Nonoshita T, Shioyama Y, Nakamura K *et al.* Concurrent chemoradiotherapy with S-1 for T2N0 glottic squamous cell carcinoma. *J Radiat Res* 2010;**51**:481–4.
22. Nakayama M, Hayakawa K, Okamoto M *et al.* Phase I/II trial of concurrent use of S-1 and radiation therapy for T2 glottic cancer. *Jpn J Clin Oncol* 2010;**40**:921–6.
23. Tsukuda M, Ishitoya J, Mikami Y *et al.* Analysis of feasibility and toxicity of concurrent chemoradiotherapy with S-1 for locally advanced squamous cell carcinoma of the head and neck in elderly cases and/or cases with comorbidity. *Cancer Chemother Pharmacol* 2009;**64**:945–52.
24. Tahara M, Minami H, Kawashima M *et al.* Phase I trial of chemoradiotherapy with the combination of S-1 plus cisplatin for patients with unresectable locally advanced squamous cell carcinoma of the head and neck. *Cancer Sci* 2011;**102**:419–24.
25. Ohashi T, Ohnishi M, Tanahashi S *et al.* Efficacy and toxicity of concurrent chemoradiotherapy with nedaplatin and S-1 for head and neck cancer. *Jpn J Clin Oncol* 2011;**41**:348–52.
26. Nakamura K, Tahara M, Kiyota N *et al.* Phase II trial of concurrent chemoradiotherapy with S-1 plus cisplatin in patients with unresectable locally advanced squamous cell carcinoma of the head and neck: Japan Clinical Oncology Group Study (JCOG0706). *Jpn J Clin Oncol* 2009;**39**:460–3.

Analysis and results of Ku and XRCC4 expression in hypopharyngeal cancer tissues treated with chemoradiotherapy

JYUNICHI HAYASHI[1], KOH-ICHI SAKATA[1], MASANORI SOMEYA[1], YOSHIHISA MATSUMOTO[3], MASAAKI SATOH[4], KENSEI NAKATA[1], MASAKAZU HORI[1], MASARU TAKAGI[1], ATSUSHI KONDOH[2], TETSUO HIMI[2] and MASATO HAREYAMA[1]

Departments of [1]Radiology, and [2]Otolaryngology, Sapporo Medical University, School of Medicine, Hokkaido; [3]Tokyo Institute of Technology, Research Laboratory for Nuclear Reactors, Tokyo; [4]Division of Clinical Pathology, NTT Sapporo Hospital, Sapporo, Japan

Received December 30, 2011; Accepted March 23, 2012

DOI: 10.3892/ol.2012.674

Abstract. DNA double-strand break (DSB) is one of the most serious forms of damage induced by ionizing irradiation. Non-homologous end-joining (NHEJ) is a key mechanism of DNA DSB repair. The immunohistochemical analysis of proteins involved in NHEJ may have potential as a predictive assay for tumor radiosensitivity. We examined the correlation between the expression of proteins involved in DNA DSB in biopsy specimens and the results of chemoradiotherapy in hypopharyngeal cancers. Fifty-seven patients with previously untreated squamous cell carcinoma of the hypopharynx were treated between March 2002 and December 2009. Most patients (75%) had stage III or IV disease. The chemotherapy consisted of cisplatin plus 5FU or S-1. A tumor dose of 50 Gy was usually administered to the primary tumor and regional lymph nodes. Doses of 10-20 Gy were usually added to the primary tumor with reduced fields after 50 Gy. The 5-year disease-free survival rate was 100% for patients in stage I, 90% in stage II, 64% in stage III and 50% in stage IV. In stages I-III, patients with a lower expression of Ku70 or XRCC4 tended to have better locoregional control. These results indicated that a lower expression of Ku70 or XRCC4 may be correlated with higher radiosensitivity. Two patients had distant metastasis alone, of which one had 0% expression of Ku70 and the other had 0% expression of Ku86. The absence of Ku70 or Ku86 expression indicates low DNA-PK activity. Low DNA-PK activity due to a low expression of Ku may result in the genetic alteration of cancer cells, leading to a higher tendency of distant metastasis. This finding suggests that proteins involved in NHEJ may have an impact on the treatment results of chemoradiotherapy in hypopharyngeal cancer.

Correspondence to: Dr Koh-ichi Sakata, Department of Radiology, Sapporo Medical University, School of Medicine, S1W16, Chuo-Ku, Sapporo 060-8543, Japan
E-mail: sakatako@sapmed.ac.jp

Key words: hypopharyngeal cancer, Ku70, Ku86, XRCC4, Ki-67, immunohistochemical staining

Introduction

Hypopharyngeal carcinoma is a difficult carcinoma to treat due to the fact that it is often diagnosed at a late stage and that it has an aggressive natural history. The standard operation is a total pharyngolaryngectomy. This procedure can have a negative impact on the well-being of patients as it involves tracheotomy and loss of natural voice, which may lead to social isolation, loss of employment and depression. Chemoradiotherapy (radiotherapy plus concurrent chemotherapy) has become the standard of care for patients with unresectable squamous cell carcinoma of the head and neck (1) and for organ preservation (2,3).

The repair of various types of DNA damage is critical for cell survival. Of these, DNA double-strand break (DSB) is understood to be one of the most serious forms of damage induced by DNA-damaging agents such as ionizing irradiation (4). Non-homologous end-joining (NHEJ) is a key mechanism of DNA DSB repair (5). In the NHEJ pathway, DSBs are rejoined at an appropriate chromosomal end, either directly or following DNA end processing, and DNA-dependent protein kinase (DNA-PK) is important in DNA DSB repair by NHEJ throughout the cell cycle (6). DNA-PK is a serine/threonine kinase, which is composed of the DNA-PK catalytic subunit (DNA-PKcs) and the heterodimer of Ku70 and Ku86. DNA-PK binds DSBs in DNA, and phosphorylates and activates DNA-binding protein, including XRCC4 and DNA ligase IV, p53 and several transcription factors. Subsequently, ligase IV repairs DNA DSB (7). Therefore, DNA-dependent protein kinase (DNA-PK) is important in DNA DSB repair. The immunohistochemical analysis of proteins involved in DNA DSB repair such as Ku70, Ku86 and XRCC4 may have potential as a predictive assay for tumor radiosensitivity (8,9).

In this study, we investigated the correlation between the expression of proteins involved in DNA DSB and the results of chemoradiotherapy for hypopharyngeal cancers in patients admitted to the Sapporo Medical University. We also examined

Table I. The treatment results according to stage.

Stage	Number of patients	Locoregional recurrence alone	Locoregional recurrence and distant metastasis	Distant metastasis alone
I	4	0	0	0
II	10	1	0	0
III	8	0	1	1
IV	35	10	6	1

the expression of Ki-67, a nuclear protein that is expressed in cycling cells.

Patients and methods

Patients. Fifty-seven Japanese patients with previously untreated squamous cell carcinoma of the hypopharynx were treated at the Sapporo Medical University between March 2002 and December 2009.

The patient population consisted of 48 men and 9 women. The mean age was 63 years (range, 33-82). The distribution according to the subsites of the hypopharynx was 48 piriform sinus, 7 postcricoid area and 2 posterior pharyngeal wall. With regard to TNM stage (7th edition), 4 patients had stage I disease, 10 had stage II, 8 had stage III and 35 had stage IV disease (Table I). Most patients (75%) had stage III or IV disease.

Patients with distant metastasis at the first admission were excluded from this study.

This study was approved by the ethics committee of Sapporo University. Patient consent was obtained either from the patient or the patient's family.

Treatments. In 51 of the 57 patients, chemotherapy was administered concurrently with radiotherapy. Six patients were treated with radiotherapy alone. The chemotherapy consisted of FP (cisplatin plus 5FU) or S-1. FP was used in 39 patients and S-1 in 12 patients. FP consisted of cisplatin 40-60 mg/m^2 intravenously and 5FU 400-700 mg/body/day for 4 days by continuous venous infusion. S-1 (50-80 mg/body) was orally administered during periods of radiotherapy.

Radiation was administered using a 4 MV photon linear accelerator. The primary tumor, jugular and retropharyngeal nodes were treated with lateral parallel-opposed photon fields. An appositional anterior field was used to irradiate the supraclavicular and paratracheal nodes. A tumor dose of 50 Gy (25 fractions/5 weeks) was administered to the primary tumor and regional lymph nodes. Doses of 10-20 Gy were usually added to the primary tumor with reduced fields after 50 Gy.

Immunohistochemical staining of various proteins in hypopharyngeal cancer tissues. Formalin-fixed, paraffin-embedded specimens from biopsy were used. Immunohistochemical staining was carried out using methods described in a previous study (10). Anti-Ku70, Ku86 or XRCC4 rabbit polyclonal antisera, which have been described previously (10,11), were used. Ki-67 staining was performed with MIB-1 monoclonal rabbit antibody (Dako, Copenhagen, Denmark) using methods described previously (12). The number of cells that stained positive for Ku70, Ku86, XRCC4 and Ki-67 were determined by scoring 3 microscopic fields of 300 tumor cells each, without prior knowledge of radiosensitivity or treatment outcome, and determining the percentages of cells that were positive for the expression of Ku70, Ku86, XRCC4 and Ki-67.

Statistical analysis. The median follow-up time to the last contact or mortality was 30 months, with a range of 0 to 93 months. The cut-off for analysis was November 2011. Patients alive at the cut-off date had a median follow-up time of 45 months. Overall and disease-free survival were calculated by the Kaplan-Meier method. Differences were analyzed by the log-rank test. A significance level of 0.05 was used throughout. Locoregional recurrence refers to recurrence in the hypopharynx and/or regional lymph nodes.

Results

Overall and disease-free survival rates. The overall 5-year survival rate in patients treated with chemoradiotherapy was 100% in stage I, 83% in stage II, 30% in stage III and 50% in stage IV (Fig. 1A). The difference in the overall 5-year survival between stages I-II and stages III-IV was significant (P=0.02). The 5-year disease-free survival rate in patients treated with chemoradiotherapy was 100% in stage I, 90% in stage II, 64% in stage III, and 50% in stage IV (Fig. 1B). The difference in disease-free survival between stages I-II and stages III-IV was significant (P=0.02).

Treatment results according to stage. Table I shows the treatment results according to stage. Only 3 of 22 patients experienced locoregional recurrence and/or distant metastasis in stages I-III compared to 17 of 35 patients in stage IV. Most patients with distant metastasis also experienced locoregional recurrence, although two patients had distant metastasis alone.

Immunohistochemical staining. The staining of Ku70, Ku86, XRCC4 and Ki-67 was nuclear with none of the normal epithelial cells or malignant cells exhibiting cytoplasmic or membrane immunoreactivity. The staining was diffuse throughout the cell nucleus (Fig. 2).

Analysis of results of immunohistology and survival. The percentage of cells that expressed Ku70, Ku86, XRCC4 and Ki-67 in different tumors was analyzed (Table II).

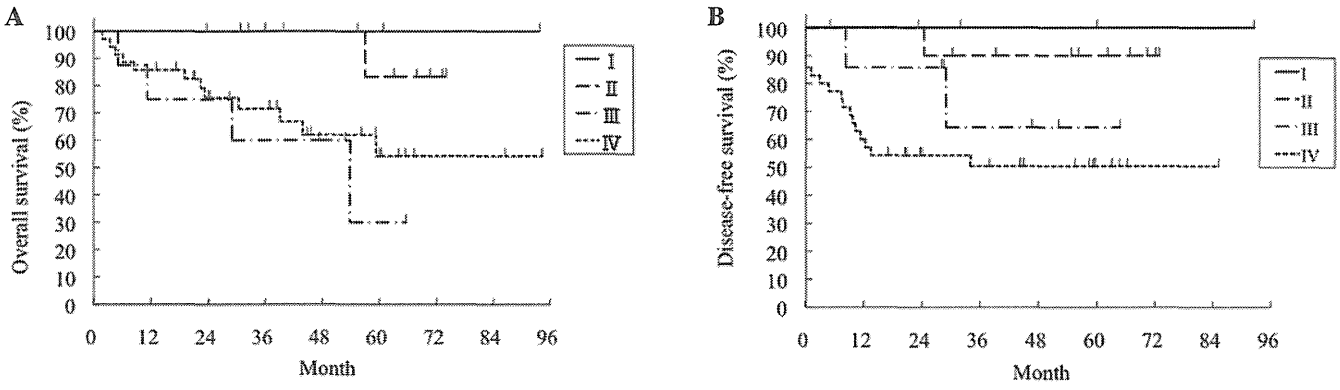

Figure 1. (A) Overall and (B) disease-free survival in patients with hypopharyngeal cancer according to stage.

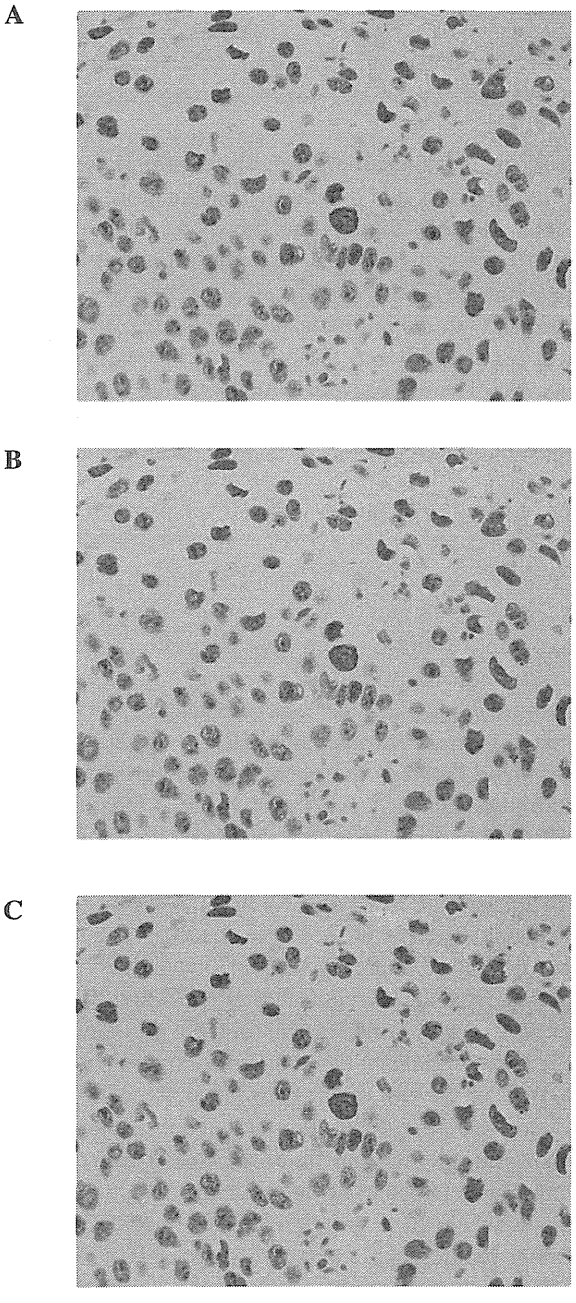

Figure 2. Expression of (A) Ku70, (B) Ku86 and (C) XRCC4 antigen in hypopharyngeal cancer tissues. Original magnification, x400.

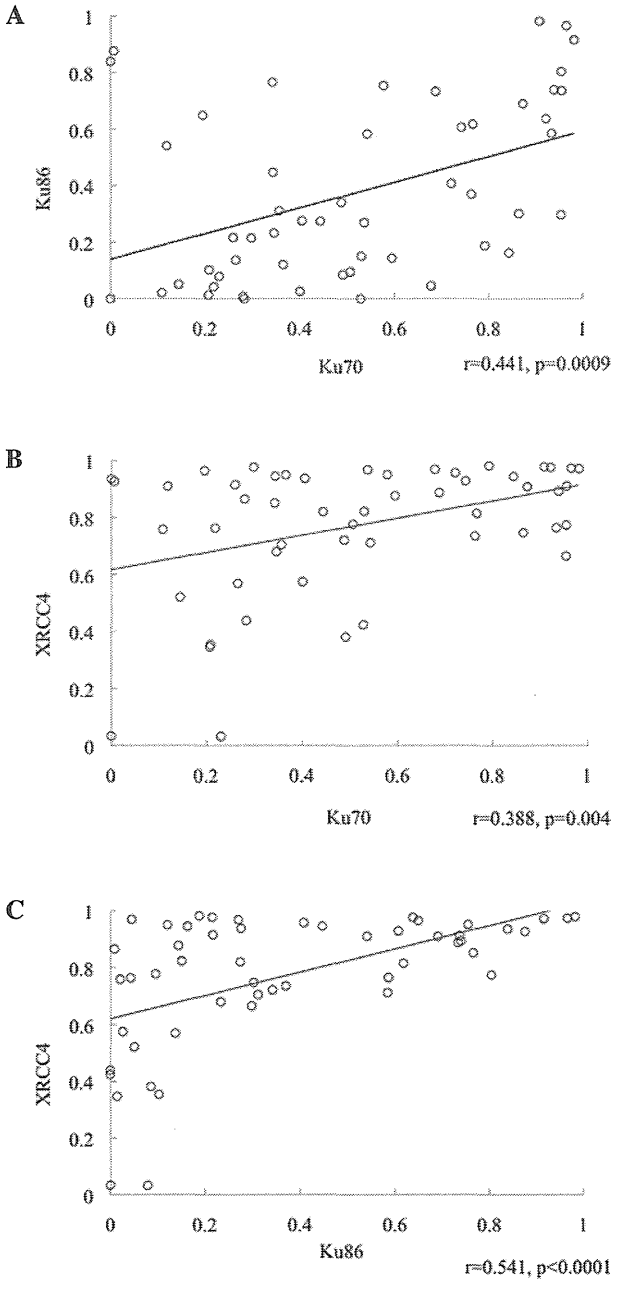

Figure 3. Correlation between the expression of (A) Ku70 and Ku86. (B) Ku70 and XRCC4 and (C) Ku86 and XRCC4.

Table II. The percentage of cells that expressed Ku70, Ku86, XRCC4 and Ki-67.

Expression	Mean ± SD (%)	Median (%)	Range (%)
Ku70	52±30	50	0-98
Ku86	37±31	29	0-98
XRCC4	77±23	86	33-98
Ki-67	37±23	31	1.4-97

Table III. The correlation between the expression of Ku70 and locoregional control according to stage.

A, Stages I, II and III

Percentage of Ku70 positivity	Number of patients	Number of recurrences	Recurrence rate (%)
<35%	10	0	0
>35%	9	2	22

B, Stage IV

Percentage of Ku70 positivity	Number of patients	Number of recurrences	Recurrence rate (%)
<35%	9	3	33
>35%	23	11	48

Table IV. The correlation between the expression of XRCC4 and locoregional control according to stage.

A, Stages I, II and III

Percentage of XRCC4 positivity	Number of patients	Number of recurrences	Recurrence rate (%)
<78%	7	0	0
>78%	11	2	18

B, Stage IV

Percentage of XRCC4 positivity	Number of patients	Number of recurrences	Recurrence rate (%)
<78%	9	5	56
>78%	23	10	43

We examined whether there was a correlation between the expression levels of proteins involved in NHEJ. A significant correlation was found between the percentage of cells expressing Ku70 and Ku86 (r=0.44; P=0.009; Fig. 3A), Ku70 and XRCC4 (r=0.39; P=0.004; Fig. 3B), and Ku86 and XRCC4 (r=0.54; P<0.0001; Fig. 3C).

The mean percentage of cells expressing Ku70 in the local control group was 49% and that in the local failure group was 57%. The mean percentage of cells expressing Ku86 in the local control group was 39% and that in the local failure group was 34%. The mean percentage of cells expressing XRCC4 in the local control group was 76% and that in the local failure group was 79%. The mean percentage of cells expressing Ki-67 in the local control group was 35% and that in the local failure group was 41%.

An analysis of the correlation between the expression of these proteins and locoregional control was performed according to stage. In stages I-III, patients with a lower expression of Ku70 (<35%) tended to have better locoregional control (Table III). In stages I-III, patients with a lower expression of XRCC4 (<78%) tended to have better locoregional control (Table IV). However, this tendency in Ku70 and XRCC4 was not significant due to the small numbers. There was no such tendency in patients with stage IV (Tables III and IV).

We also analyzed the correlation between the expression of Ku70, Ku86, XRCC4 and Ki-67 and distant metastasis. Nine patients experienced distant metastasis. In seven patients the distant metastasis was accompanied by locoregional recurrence but two patients had distant metastasis alone (Table I). In patients with both distant metastasis and locoregional recurrence, there was no apparent correlation between the expression of these proteins and distant metastasis. By contrast, in two patients with distant metastasis alone, one patient had 0% expression of Ku70 and the other had 0% expression of Ku86 (Fig. 3A). There were four patients with 0% expression of Ku70 or Ku86. None of the four patients experienced locoregional recurrence. Two patients developed distant metastasis.

Discussion

The estimates of overall and disease-free survival at 3 years in all patients were 78 and 63%, respectively (Fig. 1A and B). These treatment results were comparable with other studies using chemoradiotherapy (13,14).

We examined whether there was a correlation between the expressions of proteins involved in NHEJ. A significant correlation was found between the percentage of cells expressing Ku70 and Ku86 (Fig. 3A), Ku70 and XRCC4 (Fig. 3B), and Ku86 and XRCC4 (Fig. 3C). The results of Ku70 and Ku86 were in agreement with our previous results, demonstrating that the expression of Ku70 and Ku86 paralleled each other in breast cancer tissues (15). These results indicated that there was a concerted expression of Ku70 and Ku86 in breast cancer tissues. Hosoi *et al* reported that Ku70 and Ku86 have consensus Sp1 recognition elements in their promoter region and that Sp1 may influence the concerted expression of Ku70 and Ku86 (16). To the best of our knowledge, the correlation of the expression of XRCC4 with that of Ku70 or Ku86 is a new finding. However, the mechanism of the concerted expression of these proteins remains to be determined.

Patients with a lower expression of Ku70 or XRCC4 tended to have better locoregional control in stages I-III (Table III). Komuro *et al* reported results of 96 patients with advanced rectal carcinoma treated with preoperative radiotherapy (8). The lower expression of Ku70 or Ku86 in preradiation biopsy specimens of tumor samples was correlated with better objec-

tive responses, suggesting that low expression of Ku70 or Ku86 may be correlated with high radiosensitivity.

There was no such correlation between the expression of Ku70 or XRCC4 and locoregional control in patients with stage IV (Tables II and III). Patients with stage IV had a large primary tumor and/or large lymph node metastases. In such a situation, the large number of tumor cells and hypoxic tumor cells may affect radiocurability and obscure the effect of Ku70 or XRCC4 expression.

Ki-67 is a nuclear protein that is expressed in cycling cells. For patients treated with radiotherapy, the tumors with a high Ki-67 labeling index demonstrated good local control in squamous cell carcinomas of the head and neck (17), esophageal cancer (18) and uterine cervical cancer (19). However, no such correlation was found between the Ki-67 labeling index and locoregional control of hypopharyngeal cancer treated with chemoradiotherapy in our results. This observation indicated that chemoradiotherapy may be effective for tumors that included non-cycling cells.

There were two patients with distant metastasis alone, one of whom had 0% expression of Ku70 and the other a 0% expression of Ku86. There were four patients with 0% expression of Ku70 or Ku86 (Fig. 2A). None of the four patients experienced locoregional recurrence but two developed distant metastasis alone. These results may be associated with our previous results which demonstrated that breast cancer cells with a lower expression of Ku70 or Ku86 had aggressive cancer phenotypes such as a higher nuclear grade and positive axillary lymph node metastasis (15). Genes involved in DNA DSB repair are involved in the maintenance of genomic stability (20). We previously demonstrated that DNA-PK activity is associated with chromosomal instability (21). An absence of Ku70 or Ku86 expression indicates low DNA-PK activity. Such low DNA-PK activity resulted in the genetic alteration of cancer cells, leading to higher tendency of distant metastasis.

In conclusion, patients with a lower expression of Ku70 or XRCC4 tended to have better locoregional control in stages I-III, but there was no such tendency in patients with stage IV. In two patients with distant metastasis alone, one patient had 0% expression of Ku70 and the other had 0% expression of Ku86. This finding suggests that proteins involved in NHEJ may have an impact on the treatment results of chemoradiotherapy in hypopharyngeal cancer.

Acknowledgements

The study was supported in part by a Grant-in-Aid for Scientific Research from the Ministry of Education, Culture, Sports, Science and Technology, Japan and by a grant from the Program for Developing the Supporting System for Upgrading Education and Research in Sapporo Medical University.

References

1. Adelstein DJ, Li Y, Adams GL, *et al*: An intergroup study phase III comparison of standard radiation therapy and two schedules of concurrent chemoradiotherapy in patients with unresectable squamous cell head and neck cancer. J Clin Oncol 21: 92-98, 2003.
2. Denis F, Garaud P, Bardet E, *et al*: Final results of the 94-01 French Head and Neck Oncology and Radiotherapy Group randomized trial comparing radiotherapy alone with concomitant radiochemotherapy in advanced-stage oropharynx carcinoma. J Clin Oncol 22: 69-76, 2004.
3. Forastiere AA, Goepfert H, Maor M, *et al*: Concurrent chemotherapy and radiotherapy for organ preservation in advanced laryngeal cancer. N Engl J Med 349: 2091-2098, 2003.
4. Hall EJ: DNA strand breaks and chromosomal aberrations. In: Radiobiology for the Radiologist. Hall EJ and Giaccia AM (eds). 6th edition. Lippincott Williams & Wilkins, Philadelphia, pp16-29, 2006.
5. Polo SE and Jackson SP: Dynamics of DNA damage response proteins at DNA breaks: a focus on protein modification. Gene Dev 25: 409-433, 2011.
6. Lees-Miller SP: The DNA-dependent protein kinase, DNA-PK: 10 years and no ends in sight. Biochem Cell Biol 74: 503-512, 1996.
7. Jeggo PA: Identification of genes involved in repair of DNA double-strand breaks in mammalian cells. Radiat Res 150: S80-S91, 1998.
8. Komuro Y, Watanabe T, Hosoi Y, *et al*: The expression pattern of Ku correlates with tumor radiosensitivity and disease free survival in patients with rectal carcinoma. Cancer 95: 1199-1205, 2002.
9. Zhao HJ, Hosoi Y, Miyachi H, *et al*: DNA-dependent protein kinase activity correlates with Ku70 expression and radiation sensitivity in esophageal cancer cell lines. Clin Cancer Res 6: 1073-1078, 2000.
10. Sakata K, Matsumoto Y, Tauchi H, *et al*: Expression of genes involved in repair of DNA double-strand breaks in normal and tumor tissues. Int J Radiat Oncol Biol Phys 49: 161-167, 2001.
11. Kamdar RP and Matsumoto Y: Radiation-induced XRCC4 association with chromatin DNA analyzed by biochemical fractionation. J Radiat Res 51: 303-313, 2010.
12. Sakata K, Someya M, Nagakura H, *et al*: Brachytherapy for oral tongue cancer: an analysis of treatment results with various biological markers. Jpn J Clin Oncol 38: 402-407, 2008.
13. Pointreau Y, Garaud P, Chapet S, *et al*: Randomized trial of induction chemotherapy with cisplatin and 5-fluorouracil with or without docetaxel for larynx preservation. J Natl Cancer Inst 101: 498-506, 2009.
14. Posner MR, Hershock DM, Blajman CR, *et al*: Cisplatin and fluorouracil alone or with docetaxel in head and neck cancer. New Engl J Med 25: 1705-1715, 2007.
15. Someya M, Sakata K, Matsumoto Y, Satoh M, Narimatsu H and Hareyama M: Immunohistochemical analysis of Ku70/86 expression of breast cancer tissues. Oncol Rep 18: 1483-1487, 2007.
16. Hosoi Y, Watanabe T, Nakagawa K, *et al*: Up-regulation of DNA-dependent protein kinase activity and Sp1 in colorectal cancer. Int J Oncol 25: 461-468, 2004.
17. Raybaud-Diogene H, Fortin A, Morency R, Roy J, Monteil RA and Tetu B: Markers of radioresistance in squamous cell carcinomas of the head and neck: a clinicopathologic and immunohistochemical study. J Clin Oncol 15: 1030-1038, 1997.
18. Okuno Y, Nishimura Y, Kashu I, Ono K and Hiraoka M: Prognostic values of proliferating cell nuclear antigen (PCNA) and Ki-67 for radiotherapy of oesophageal squamous cell carcinomas. Br J Cancer 80: 387-395, 1999.
19. Nakano T and Oka K: Differential values of Ki-67 index and mitotic index of proliferating cell population. An assessment of cell cycle and prognosis in radiation therapy for cervical cancer. Cancer 72: 2401-2408, 1993.
20. Burma S, Chen BPC and Chen DJ: Role of non-homologous end joining (NHEJ) in maintaining genomic integrity. DNA Repair 5: 1042-1048, 2006.
21. Someya M, Sakata K, Matsumoto Y, *et al*: The association of DNA-dependent protein kinase activity with chromosomal instability and risk of cancer. Carcinogenesis 27: 117-122, 2006.

International Journal of
Radiation Oncology
biology • physics

www.redjournal.org

Physics Contribution

Functional Image-Guided Radiotherapy Planning in Respiratory-Gated Intensity-Modulated Radiotherapy for Lung Cancer Patients With Chronic Obstructive Pulmonary Disease

Tomoki Kimura, M.D., Ikuno Nishibuchi, M.D., Yuji Murakami, M.D., Ph.D., Masahiro Kenjo, M.D., Yuko Kaneyasu, M.D., Ph.D., and Yasushi Nagata, M.D., Ph.D.

Department of Radiation Oncology, Hiroshima University, Graduate School of Biomedical Sciences, Hiroshima City, Japan

Received Feb 16, 2011, and in revised form Jun 27, 2011. Accepted for publication Aug 5, 2011

Summary

We investigated the incorporation of functional lung image-derived low attenuation area (LAA) based on 4D-CT into respiratory-gated IMRT or VMAT in treatment planning for lung cancer patients with COPD. Respiratory-gated plans (anatomic and functional) were compared and the lung V20 found to be lower in the functional than the anatomic plan through a reduction in MLD. Functional image-guided planning appears to be helpful in preserving functional lung in lung cancer patients with COPD.

Purpose: To investigate the incorporation of functional lung image-derived low attenuation area (LAA) based on four-dimensional computed tomography (4D-CT) into respiratory-gated intensity-modulated radiotherapy (IMRT) or volumetric modulated arc therapy (VMAT) in treatment planning for lung cancer patients with chronic obstructive pulmonary disease (COPD).

Methods and Materials: Eight lung cancer patients with COPD were the subjects of this study. LAA was generated from 4D-CT data sets according to CT values of less than than −860 Hounsfield units (HU) as a threshold. The functional lung image was defined as the area where LAA was excluded from the image of the total lung. Two respiratory-gated radiotherapy plans (70 Gy/35 fractions) were designed and compared in each patient as follows: Plan A was an anatomical IMRT or VMAT plan based on the total lung; Plan F was a functional IMRT or VMAT plan based on the functional lung. Dosimetric parameters (percentage of total lung volume irradiated with ≥20 Gy [V20], and mean dose of total lung [MLD]) of the two plans were compared.

Results: V20 was lower in Plan F than in Plan A (mean 1.5%, $p = 0.025$ in IMRT, mean 1.6%, $p = 0.044$ in VMAT) achieved by a reduction in MLD (mean 0.23 Gy, $p = 0.083$ in IMRT, mean 0.5 Gy, $p = 0.042$ in VMAT). No differences were noted in target volume coverage and organ-at-risk doses.

Conclusions: Functional IGRT planning based on LAA in respiratory-guided IMRT or VMAT appears to be effective in preserving a functional lung in lung cancer patients with COPD.
© 2012 Elsevier Inc.

Keywords: Functional imaging, 4D-CT, IMRT, COPD

Reprint requests to: Tomoki Kimura, M.D., Department of Radiation Oncology, Hiroshima University, Graduate School of Biomedical Sciences, 1-2-3, Kasumi, Minami-ku, Hiroshima City, 734-8551, Japan. Tel: 81-82-257-1545; Fax: 81-82-257-1546; E-mail: tkkimura@hiroshima-u.ac.jp

This work was supported in part by a Grant-in-Aid for Scientific Research from the Ministry of Education, Culture, Sports, Science and Technology of Japan (Grant no. 22591385), and a Grant-in-Aid for Scientific Research from the Association for Nuclear Technology in Medicine.

This work was partly presented at the 52nd Annual Meeting of the American Society of Radiation Oncology, San Diego, CA, Oct 31—Nov 4, 2010.

Conflict of interest: none.

Int J Radiation Oncol Biol Phys, Vol. 82, No. 4, pp. e663—e670, 2012
0360-3016/$ - see front matter © 2012 Elsevier Inc. All rights reserved.
doi:10.1016/j.ijrobp.2011.08.016

Introduction

One of the most severe complications in radiotherapy for lung cancer is radiation pneumonitis (RP). Reduction of the incidence of severe RP requires a reduction of the lung dose, such as V20 which is defined as the percentage of pulmonary volume irradiated to ≥20 Gy. It is also one of the significant dosimetric risk factors for the incidence and severity of RP (1). Chronic obstructive pulmonary disease (COPD) is a recognized risk factor for RP (2). There has been a worldwide increase of the prevalence of COPD and as the population ages, the incidence of COPD is expected to increase (3). Pulmonary emphysema (PE) is a subtype of COPD, and defined pathologically as a group of diseases that demonstrate anatomic alterations in the lung, characterized by enlargement of airspaces distal to the terminal bronchioles, accompanied by destructive changes of alveolar walls (4). These lesions are seen as low-attenuation areas (LAAs) on CT scans, and are established findings on the imaging diagnosis of COPD (5, 6). Kimura *et al.* reported a correlation between the incidence of RP and the extent of LAAs in the whole lung fields (7). From these results, the functional lung image-derived LAA based on four-dimensional computed tomography (4D-CT) was developed for planning of radiation treatment to reduce the risk of RP in patients with COPD.

Several authors have described functional imaging modalities for planning of radiation treatment, such as ventilation imaging with 4D-CT (8) and single-photon emission computed tomography (SPECT) lung perfusion imaging (9). All of these authors showed that functional lung regions could be identified with imaging and then avoided with IMRT treatment planning techniques. Matsuoka (6) suggested that paired inspiratory and expiratory CT imaging can be used to define LAA volumes in patients with COPD. Therefore, these two approaches were combined in order to address the respiratory problem. This study investigated the ability of functional lung image-derived LAA based on 4D-CT, and its incorporation into respiratory-gated intensity-modulated radiotherapy (IMRT) or volumetric modulated arc therapy (VMAT) in treatment planning for lung cancer patients with COPD.

Methods and Materials

Patient background

In this study, 8 male patients with lung cancer were enrolled who had undergone 4D-CT scanning and definitive radiotherapy at Hiroshima University from 2009 to 2010. Pathological diagnosis, stage (Union International Contre le Cancer [UICC] 7th edition), and the primary tumor location are summarized in Table 1. All patients received [18F] fluorodeoxyglucose–positron emission tomography (FDG-PET) for staging.

Functional lung image-derived LAA based on 4D-CT

At first, 4D-CT scans were acquired with 2.5-mm-thick slices using multi detector-row CT (MDCT; LightSpeed, GE Medical systems, Waukesha, WI) in cine mode with the Varian Real-time Position Management (RPM) Respiratory Gating system (Varian Medical Systems, Palo Alto, CA). After image acquisition, the CT image data set was sorted into 10-phase bins of the respiratory cycle, and phase by phase evaluation was performed on a workstation (AdvantageSim, GE Healthcare, Princeton, NJ). The 10-phase set consisted of 0 to 90% in steps of 10%, and 0 or 90% was in the end-inspiratory phase and 50% in the end-expiratory phase. All 10-phase CT data sets were imported into the Eclipse treatment planning system (Varian Medical Systems, Palo Alto, CA). Several authors reported that the threshold CT value for the detection and quantification of LAA ranged from -850 to -950 HU (10, 11). Matsuoka *et al.* concluded that the threshold of -860 HU correlated closely with airway dysfunction in COPD on paired inspiratory and expiratory CT (6). Therefore LAAs were generated from 10-phase 4D-CT data sets according to CT values lower than -860 Hounsfield units (HU) as a threshold on Eclipse.

For respiratory gated planning in this study, three expiratory phases (40-60%) were selected with the phase gating method. Figure 1 shows the three steps involved in making the functional lung image-derived LAA based on 4D-CT in Case 1: *(1)* acquisition of LAA at each phase (the threshold of -860HU); *(2)* fusion of LAA at three expiratory phases (40–60%), and trimming the ROI as LAA image (40–60%); and *(3)* the functional lung image was defined as the area where LAA image (40–60%) was excluded from fusion images of the total lung volumes on each of the 40–60% phases.

This technique did not use any sort of deformable image registration algorithm in any of the steps.

Respiratory gated IMRT and VMAT planning with functional lung image

In this simulation study, two respiratory-gated radiotherapy plans were designed and compared for each patient as follows: *(1)* Plan A was an anatomical IMRT or VMAT plan based on the total lung; *(2)* Plan F was a functional IMRT or VMAT plan based on the functional lung. RapidArc (Varian Medical Systems, Palo Alto, CA) was used as VMAT. In this study, IMRT was defined as fixed, nonrotational IMRT, and VMAT was defined as rotational IMRT. All dose calculations were done on the full expiration (50%) phase.

For target delineation of each plan, a physician delineated the target volume on each 10-phase CT image. Gross tumor volume (GTV) included the primary tumor and metastatic lymph nodes, and clinical target volume (CTV) margin of 3 to 5 mm was added to GTV according to the pathology. Elective nodal irradiation was omitted (so-called "involved-field"). Internal target volume (ITV)

Table 1 Characteristics of study patients

Case patient	Age (y)	Sex	Histology	TNM	Stage	Tumor location
1	81	M	Non-small	T2aN1M0	IIB	R.S8
2	86	M	SCC	T2aN0M0	IB	L.S8
3	56	M	Adeno	T4N2M0	IIIB	R.S1
4	68	M	Small	T2aN1M0	IIB	R.S10
5	71	M	SCC	T2aN3M0	IIIB	R.S10
6	74	M	Small	T2aN2M0	IIIA	L.S8
7	68	M	SCC	T3N2M0	IIIA	R.S6
8	84	M	Non-small	T1N0M0	IA	L.S8

Abbreviations: Non-small = non-small cell carcinoma; SCC = squamous cell carcinoma; Small = small cell carcinoma; Adeno = adenocarcionoma; F = female; M = male.

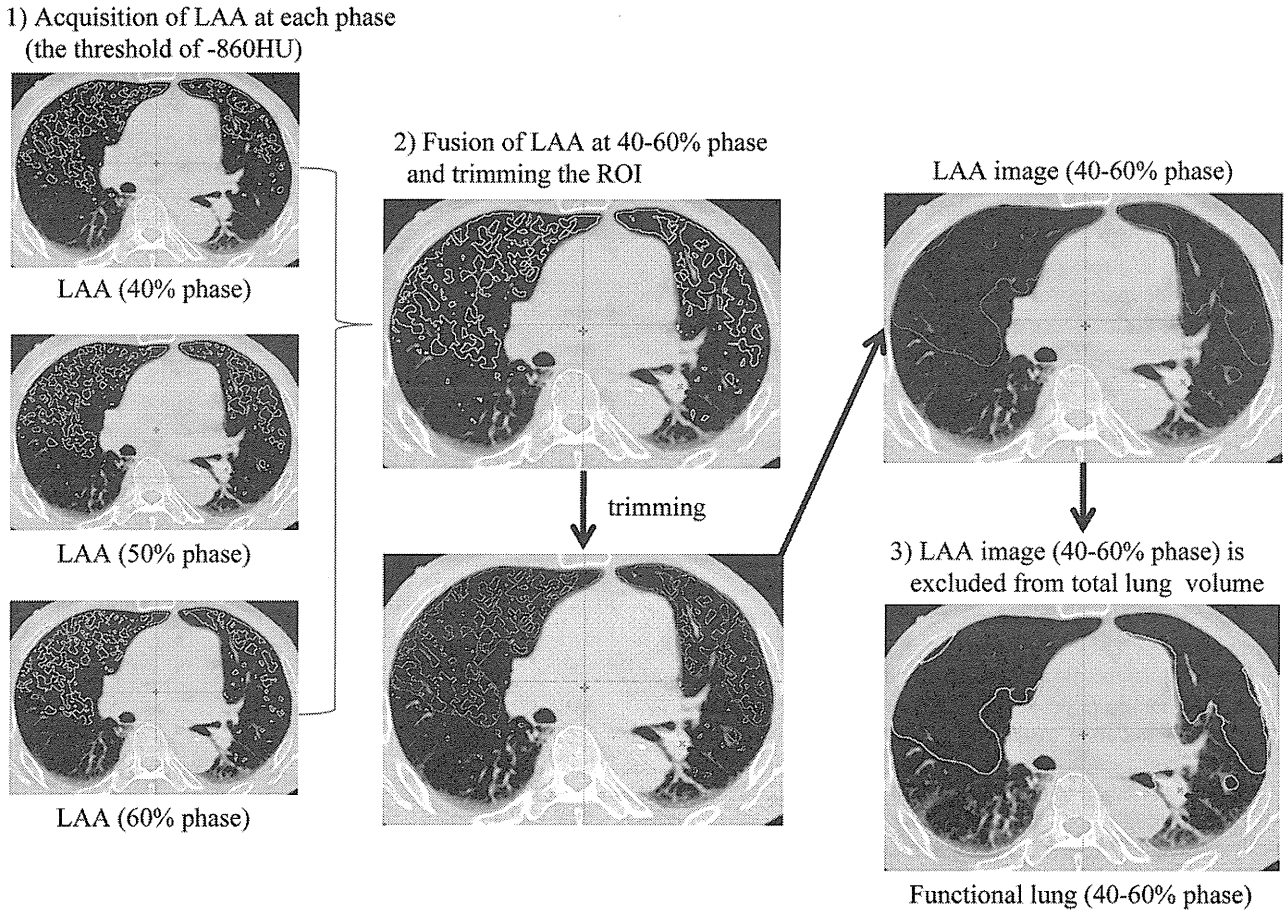

Fig. 1. Three steps to make the functional lung image-derived low attenuation area (LAA) based on four-dimensional computed tomography (4D-CT) in Case 1.

Table 2 Dose constraints for intensity-modulated radiotherapy (IMRT) and volumetric modulated arc therapy (VMAT)

	Plan A: Anatomical plan			Plan F: Functional		
	Volume (%)	Dose (cGy)	Priority	Volume (%)	Dose (cGy)	Priority
PTV						
Upper	0	7,350	70	0	7350	70
	10	7,200	70	10	7200	70
Lower	98	7,000	80	98	7000	80
	100	6,650	70	100	6650	70
Cord						
Upper	0	4,500	90	0	4500	90
Esophagus						
Upper	0	7,350	50	0	7350	50
	35	5,500	50	35	5500	50
Heart						
Upper	50	4,500	50	50	4500	50
Body						
Upper	0	7,500	50	0	7500	50
Lung						
Upper	10–30	2,000	90			
Functional lung						
Upper				10–30	2000	120
Low-functional lung (LAA†)						
Upper				10–30	2000	90

Table 3 Target (planning target volume [PTV]), normal tissue, and dosimetric characteristics of study patients

Case	PTV (cm^3)	Total lung volume (cm^3)	Functional lung volume (cm^3)	Defect size (as % of total lung)	Dose constraints of V20 or fV20
1	158.8	3354.5	1,617.6	51.8	<20%
2	228.3	2819.6	1,717.3	39.1	<10%
3	207.3	3258.1	2,302.3	29.3	<10%
4	278.4	2719.1	2,012.5	26	<30%
5	505.9	2490	2,264.1	9.1	<20%
6	256.4	2885.4	1,586.6	45	<25%
7	561.1	2517.1	1,903.4	24.4	<25%
8	62.4	3124.2	866.8	72.3	<10%
Mean	282.3	2896	1,810.4	37.1	

was defined as the sum of CTV at three expiratory phases (40-60%) in this respiratory gated planning. A planning target volume (PTV) margin of 5-10 mm was added allowing for reproducibility of respiratory motion and setup error to ITV.

The IMRT plans consisted of five coplanar fixed beams with gantry angles of 20°, 320°, 240°, 180°, and 135° at the right lung, and 340°, 40°, 120°, 180°, and 215° at the left lung. The VMAT plans consisted of two coplanar arcs with gantry angles were moved 220° from 180° to 40° in the right lung, and from 180° to 320° in the left lung in clockwise and counter clockwise directions. Treatment plans were delivered using 6-MV photons generated by a linear accelerator (Clinac iX, Varian Medical Systems, Palo Alto, CA) with continuous changes in the gantry speed, multi-leaf collimator position, and dose rate. The collimator angle was fixed at 45° throughout the arc. The same beam arrangements were used for both plans.

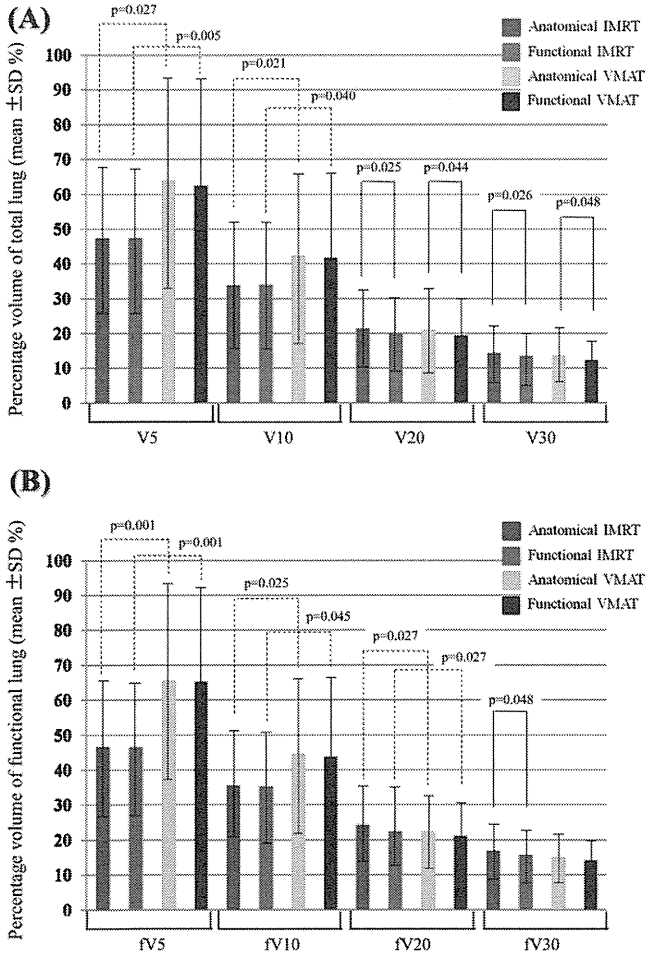

Fig. 2. Comparison of V5-30 and fV5-30 in Plans A and F using intensity-modulated radiotherapy (IMRT) and volumetric modulated arc therapy (VMAT) (mean ± SD). The *p* values shown are only for statistically significant differences.

A total dose of 70 Gy in 35 fractions to 95% of the PTV was prescribed. The prescribed dose was calculated with a heterogeneous dose calculation algorithm (the Eclipse anisotropic analytical algorithm; AAA). Table 2 shows the dose constraints for each structure. The constraints on the total lung were used in Plan A, and those on the two functional lung regions were used in Plan F. V20 or functional V20 (fV20) was calculated by lung-PTV and its dose constraints were defined as less than 10-30%. Therefore the background of patients included all stages. The minimal value of V20 which could be achieved in the anatomical plan of each patient was selected according to the field size of each patient, and the value of fV20 was also the same. Several IMRT and VMAT plans were made to maintain clinical acceptability, and the plans which most suitably satisfied the dose constraints in Table 2 were selected for Plans A and F.

Data analysis and statistical methods

The dosimetric parameters of Plans A and F using respiratory guided IMRT and VMAT planning were evaluated by examining the following: *(1)* Lung V5-30 and fV5-30: the percentage of total or functional lung volumes irradiated with ≥5 to 30 Gy; *(2)* Lung MLD and functional MLD (fMLD): mean dose to total or functional lung; *(3)* mean dose, homogeneity index (HI), and conformity index (CI) of PTV; HI = maximum dose of PTV/minimum dose to PTV; CI = treated volume/PTV; it is implied that treated volume completely encompasses the PTV; *(4)* mean or maximum dose of organ-at-risk (heart, esophagus, and spinal cord); and *(5)* monitor units for each plan.

For comparison of statistical significance, the Mantel–Haenzel χ^2 or *t*-test was used. All statistical analysis was performed using StatMate for Windows (StatMate version 4.01; ATMS, Tokyo, Japan). Statistical significance was defined as $p < 0.05$.

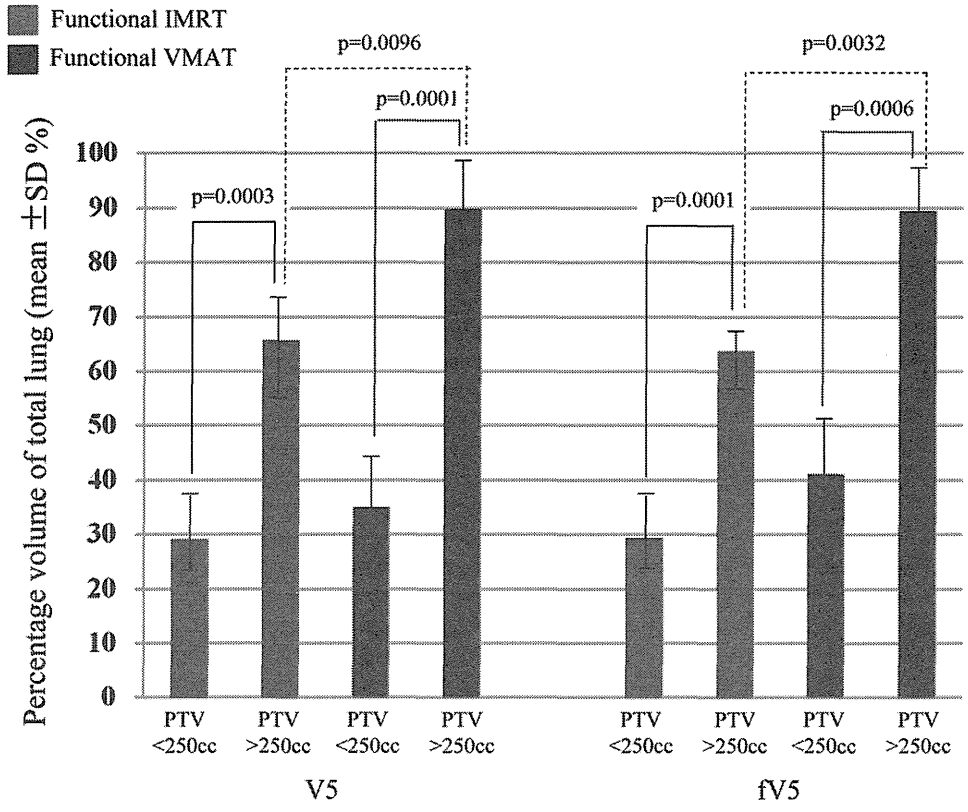

Fig. 3. Comparison of V5 and fV5 in intensity-modulated radiotherapy (IMRT) and volumetric modulated arc therapy (VMAT) of Plan F according to planning target volume (PTV). The p values shown are only for statistically significant differences.

Results

Details of target characteristics

The details of target characteristics used in both plans are presented in Table 3.

Comparison of dosimetric parameters for lung

Figs 2A and B show the mean percentage volumes of total lung (A) or functional lung (B) receiving ≥5, ≥10, ≥20 and ≥30 Gy (V5, V10, V20, V30, and fV5, fV10, fV20, fV30, respectively) for both IMRT and VMAT. Compared with Plan A, Plan F reduced V20 in IMRT (mean 1.5%, p= 0.025), in VMAT (mean 1.6%, p = 0.044), V30 in IMRT (mean 1.0%, p = 0.026), in VMAT (mean 1.3%, p = 0.048) and fV30 in IMRT (mean 1.3%, p = 0.048). Small reductions were noted in MLD (mean 0.23 Gy, p = 0.083 in IMRT, mean 0.5 Gy, p = 0.042 in VMAT) and fMLD (mean 0.3 Gy, p = 0.106 in IMRT, mean 0.5 Gy, p = 0.092 in VMAT).

On the other hand, compared with IMRT, VMAT reduced fV20 in Plan A (mean 2.0%, p = 0.027), and in Plan F (mean 1.3%, p = 0.027), but increased V5 in Plan A (mean 16.4%, p = 0.027), in Plan F (mean 15.1%, p = 0.005); V10 in Plan A (mean 8.4%, p = 0.021), in Plan F (mean 7.7%, p = 0.040); fV5 in Plan A (mean 19.0%, p = 0.001), in Plan F (mean 18.7%, p = 0.001) and fV10 in Plan A (mean 9.3%, p = 0.025), in Plan F (mean 8.4%, p = 0.045). Significant increases were also seen in MLD (mean 1.1 Gy, p = 0.013 in Plan A, mean 0.8 Gy, p = 0.010 in Plan F) and fMLD (mean 1.1 Gy, p = 0.037 in Plan A, mean 0.9 Gy, p = 0.002 in Plan F).

Fig 3 shows V5 and fV5 in IMRT and VMAT of Plan F according to PTV. Compared with PTV < 250 cc, IMRT and VMAT significantly increased V5 and fV20 in PTV ≥ 250 cc. In addition, compared with IMRT, VMAT also increased V5 and fV5 in PTV ≥ 250 cc significantly (p = 0.0096 in V5, p = 0.0032 in fV5).

Comparison of dosimetric parameters for PTV and organs at risk

Table 4 (upper) shows the dosimetric parameters for PTV, organ-at-risk and monitor units (MU) between Plans A and F. There were no differences of PTV mean dose, HI, CI, mean or maximum dose to organ-at-risk, such as heart, esophagus and spinal cord and MU between Plans A and F in both IMRT and VMAT.

Table 4 (lower) shows the dosimetric parameters for PTV, organ-at-risk and MU between IMRT and VMAT. Compared with IMRT, VMAT improved HI and CI of PTV, especially in Plan F (p = 0.040) without change in mean dose to PTV. However, there was no difference in mean or maximum doses to heart and spinal cord between IMRT and VMAT, and VMAT increased mean dose to esophagus (mean 3.9 Gy, p = 0.002 in Plan A, mean 3.6 Gy, p = 0.003 in Plan F) in both Plans A and F. However, IMRT resulted in greater MU than in VMAT in both Plans A and F (p = 0.008 and 0.003).

Figure 4 shows dose distribution in Case 4.

Table 4 Comparison of dosimetric parameters of planning target volume (PTV) and normal tissue between anatomical and functional plans, for intensity-modulated radiotherapy (IMRT) and volumetric modulated arc therapy (VMAT) (mean ± SD)

	IMRT			VMAT		
(upper)	Anatomical	Functional	*p* Value	Anatomical	Functional	*p* Value
PTV						
Mean dose (Gy)	72.6 ± 1.2	72.9 ± 0.9	0.155	72.2 ± 1.0	72.3 ± 1.1	0.629
Homogeneity index*	1.52 ± 0.08	1.59 ± 0.08	0.056	1.51 ± 0.10	1.51 ± 0.10	1
Conformity index†	2.74 ± 0.72	3.17 ± 1.07	0.128	2.44 ± 0.49	2.53 ± 0.49	0.356
Heart						
Mean dose (Gy)	19.7 ± 9.7	20.6 ± 10.6	0.214	19.1 ± 10.2	19.9 ± 11.1	0.356
Esophagus						
Mean dose (Gy)	15.6 ± 11.4	15.6 ± 11.6	0.951	19.5 ± 13.1	19.2 ± 13.2	0.522
Spinal cord						
Mean dose (Gy)	9.1 ± 6.3	9.2 ± 6.3	0.456	10.3 ± 5.4	9.9 ± 5.8	0.257
Maximum dose (Gy)	40.6 ± 21.2	40.6 ± 20.5	0.954	42.0 ± 14.6	41.1 ± 15.9	0.269
MU	786.8 ± 214.3	817.3 ± 203.1	0.378	496.5 ± 60.9	529.9 ± 56.5	0.149
	Anatomical			Functional		
(lower)	IMRT	VMAT	*p* Value	IMRT	VMAT	*p* Value
PTV						
Mean dose (Gy)	72.6 ± 1.2	72.2 ± 1.0	0.275	72.9 ± 0.9	72.3 ± 1.1	0.129
Homogeneity index*	1.52 ± 0.08	1.51 ± 0.10	0.831	1.59 ± 0.08	1.51 ± 0.10	0.077
Conformity index†	2.74 ± 0.72	2.44 ± 0.49	0.23	3.17 ± 1.07	2.53 ± 0.49	0.04
Heart						
Mean dose (Gy)	19.7 ± 9.7	19.1 ± 10.2	0.639	20.6 ± 10.6	19.9 ± 11.1	0.671
Esophagus						
Mean dose (Gy)	15.6 ± 11.4	19.5 ± 13.1	0.002	15.6 ± 11.6	19.2 ± 13.2	0.003
Spinal cord						
Mean dose (Gy)	9.1 ± 6.3	10.3 ± 5.4	0.117	9.2 ± 6.3	9.9 ± 5.8	0.281
Maximum dose (Gy)	40.6 ± 21.2	42.0 ± 14.6	0.711	40.6 ± 20.5	41.1 ± 15.9	0.888
MU	786.8 ± 214.3	496.5 ± 60.9	0.008	817.3 ± 203.1	529.9 ± 56.5	0.003

Abbreviation: MU = monitor units.
* Maximum dose of PTV/minimum dose of PTV.
† Irradiated volume that is covered by minimum dose of PTV/PTV.

Discussion

This study showed that planning of functional image-guided radiotherapy based on LAA can improve the dosimetric parameters for lung without a major change of PTV coverage and increasing other organ-at-risk doses. IMRT appears to be a good treatment planning based on favorable outcomes and maintenance of dosimetric predictors of toxicity at acceptable levels for patients who have larger tumors with difficult geometry in critical locations (12). However, inasmuch as reductions in MLD, V20, and V10 have been shown by IMRT, it can also increase the volume of lung receiving low doses, such as V5, which may potentially increase lung toxicity (13, 14). For delivering safe IMRT for lung cancer, it is important for dosimetric factors to be carefully considered. In fact, severe radiation pneumonitis may be easily induced by a lower dose in patients with COPD, which seldom comprises normal lung tissue (7). It is especially in these patients that the functional IMRT described here may contribute to minimize the effect of lower doses.

Several authors have reported on functional imaging modalities for planning of radiation treatment. Ventilation imaging is one of the modalities, which is generated from CT image volumes of the thorax representing exhale and inhale phases obtained from components of the 4D-CT sets using a deformable image registration algorithm (8, 15). Yaremko *et al.* reported generation of high functional regions, comprising the 90th percentile of the functional volume and 10% of the lung volume where the highest ventilation occurred. IMRT plans were generated using constraints on the high-functional regions. This method led to the result in which the mean dose to the high-functional region was reduced by 2.9 Gy (8). Yamamoto *et al.* also reported the effectiveness of the ventilation imaging-based functional planning (15). In their study, functional lung was divided into high-, moderate-, and low-functional regions, and the average reductions of the mean dose in the high-functional lung were 1.8 Gy for IMRT and 2.0 Gy for VMAT. This was achieved by using constraints on each region, for patients who had high-function lungs adjacent to the PTV.

SPECT lung perfusion imaging is the other functional imaging modality, which provides information about the function of pulmonary vascular and alveolar subunits. Shioyama *et al.* reported that the functional plans reduced the median dose of the 50th and 90th percentile hyperperfusion lung to 2.2 and 4.2 Gy, respectively, compared with anatomic plans by incorporating perfusion information in IMRT planning (9).

An advantage of these modalities is that several degrees of functional regions can be described according to the degree of

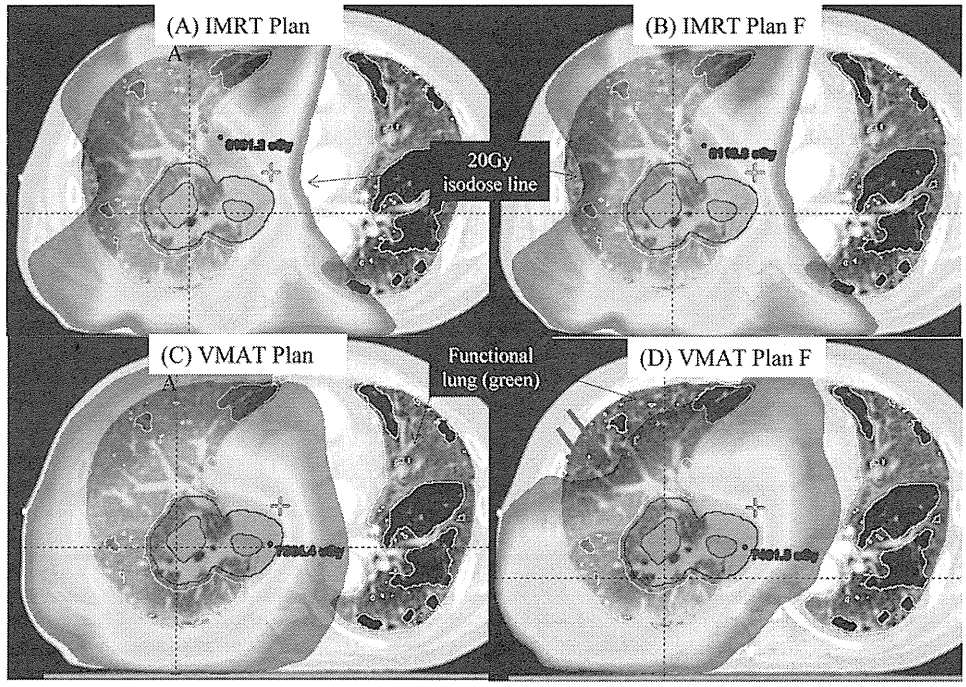

Fig. 4. Dose distribution of Case 4. (A) Intensity-modulated radiotherapy (IMRT) plan A, (B) IMRT plan F, (C) volumetric modulated arc therapy (VMAT) plan A, and (D) VMAT plan F show isodose line ≥20 Gy (blue) and functional lung area (green). The isodose line ≥20 Gy was decreased at the functional lung in VMAT Plan F (red arrows).

its regional volume change or perfusion distribution. However, the regional physiologic accuracy has not been validated in the ventilation imaging because of the uncertainty regarding the use of deformable image registration. In addition, the use of SPECT lung perfusion imaging is limited by the need for separate imaging sessions or fusions in radiotherapy planning.

The functional lung image-derived LAA based on 4D-CT of this study focused only on describing nonfunctional lung regions. The advantages of this method are as follows: *(1)* Actual lung function may be easily recognized especially in patients with COPD by using LAA-based images. *(2)* Our LAA approach can be done simply, without the need of a sophisticated deformable image registration algorithm. *(3)* This method may be less affected by respiratory motion because of the respiratory-gated technique. Consequently, there was limited description of several degrees of functional regions. However, CT quantitation using LAA is already an established tool for *in vivo* assessment of COPD, and has been correlated with pulmonary function (10, 11). Especially in CT findings of patients with COPD, LAA appears as areas of decreased lung attenuation because of an air-trapping phenomenon, which is characterized by progressive air way obstruction and airflow limitation that are not reversible with the administration of bronchodilator drugs (16). Therefore Zaporozhan *et al.* reported that PE volumes measured from expiratory MDCT scans better reflect abnormalities in pulmonary function tests in patients with severe PE than those from inspiratory scans (17). Considering the better reproducibility of lung motion, expiratory phases of 4D-CT were selected for this study. A problem remains in that 4D-CT data acquisition by this method is affected by respiratory motion. Thus, the proper thresholds of CT values for the detection and quantification of LAA and the correlations with pulmonary function using this method need to be evaluated. Nevertheless, the advantage of this respiratory gated method is that it can reduce not only the artifact of respiratory motion but also the total lung dose to a minimum.

Fixed-beam IMRT and VMAT plans were also compared. An advantage of VMAT over IMRT is the improvement of target conformity and the potential reduction in delivery time, especially in stereotactic body radiotherapy for lung cancer, which requires a large number of beams and monitor units (18). On the other hand, Schallenkamp *et al.* reported that larger volumes of lungs treated with lower doses may be more critical in predicting adverse events than smaller volumes treated with higher doses, especially when using the IMRT technique which delivers low doses of radiation to large lung volumes (19). Yamamoto *et al.* reported that functional IMRT and VMAT planning had a similar impact on each other for high-functional lung dose, PTV metrics, and doses to other critical organs (15). In our comparison with IMRT, although VMAT reduced fV20 and MU and improved HI and CI of PTV, VMAT increased the low-dose areas in both plans, especially in patients with large PTV. Increasing the low-dose area of lung using VMAT in patients with large PTV needs to be approached with caution.

The use of functional lung image-derived LAA into respiratory-gated IMRT or VMAT in planning for lung cancer patients may remove the uncertainties of quantifying LAA because of respiratory motion, and may result in further reductions of total and functional lung doses in functional planning. However, several problems need to be addressed for clinical use. Prospective clinical trials will be necessary to determine whether treatment results, such as survival and complications, are improved by using this functional avoidance treatment planning.

Conclusion

In conclusion, functional IGRT planning based on LAA in respiratory-guided IMRT or VMAT appears to be effective in

preserving a functional lung in lung cancer patients with COPD. Further investigations are needed, including those to clarify several technical problems mentioned above, and to conduct prospective clinical trials.

References

1. Graham MV, Purdy JA, Emami B, *et al.* Clinical dose-volume histogram analysis for pneumonitis after 3D treatment for non-small cell lung cancer (NSCLC). *Int J Radiat Oncol Biol Phys* 1999;45: 323–329.
2. Rancati T, Ceresoli GL, Gagliardi G, *et al.* Factors predicting radiation pneumonitis in lung cancer patients: A retrospective study. *Radiother Oncol* 2003;67:275–283.
3. Fukuchi Y, Nishimura M, Ichinose M, *et al.* COPD in Japan: The Nippon COPD Epidemiology study. *Respirology* 2004;9:458–463.
4. American Thoracic Society. Standard for the diagnosis and care of patients with chronic obstructive pulmonary disease (COPD) and asthma. *Am Rev Respir Dis* 1987;136:225–232.
5. Orlandi I, Moroni C, Camiciottoli G, *et al.* Chronic obstructive pulmonary disease: Thin-section CT measurement of airway wall thickness and lung attenuation. *Radiology* 2005;234:604–610.
6. Matsuoka S, Kurihara Y, Yagihashi K, *et al.* Quantitative assessment of air trapping in chronic obstructive pulmonary disease using inspiratory and expiratory volumetric MDCT. *AJR Am J Roentgenol* 2008;190:762–769.
7. Kimura T, Togami T, Takashima H, *et al.* Radiation pneumonitis in patients with lung and mediastinal tumors: A retrospective study of risk factors focused on pulmonary emphysema. *Br J Radiol* (in press).
8. Yaremko BP, Guerrero TM, Noyola-Martinez J, *et al.* Reduction of normal lung irradiation in locally advanced non-small cell lung cancer patients, using ventilation images for functional avoidance. *Int J Radiat Oncol Biol Phys* 2007;68:562–571.
9. Shioyama Y, Jang SY, Liu HH, *et al.* Preserving functional lung using perfusion imaging and intensity-modulated radiation therapy for advanced-stage non-small cell lung cancer. *Int J Radiat Oncol Biol Phys* 2006;68:562–571.
10. Park KJ, Bergin CJ, Clausen JL. Quantitation of emphysema with three-dimensional CT densitometry: Comparison with two-dimensional analysis, visual emphysema scores, and pulmonary function test results. *Radiology* 1999;211:541–547.
11. Gevenois PA, Vuyst PD, Sy M, *et al.* Pulmonary emphysema: Quantitative CT during expiration. *Radiology* 1996;1999: 825–829.
12. Sura S, Gupta V, Yorke E, *et al.* Intensity-modulated radiation therapy (IMRT) for inoperable non-small cell lung cancer: The Memorial Sloan-Kettering Cancer Center (MSKCC) experience. *Radiother Oncol* 2008;87:17–23.
13. Liu HH, Wang X, Dong L, *et al.* Feasibility of sparing lung and other thoracic structures with intensity-modulated radiotherapy for non-small cell lung cancer. *Int J Radiat Oncol Biol Phys* 2004;58:1268–1279.
14. Murshed H, Liu HH, Liao Z, *et al.* Dose and volume reduction for normal lung using intensity-modulated radiotherapy for advanced-stage non-small cell lung cancer. *Int J Radiat Oncol Biol Phys* 2004;58:1257–1267.
15. Yamamoto T, Kabus S, Berg JV, *et al.* Impact of four-dimensional computed tomography pulmonary ventilation imaging-based functional avoidance for lung cancer radiotherapy. *Int J Radiat Oncol Biol Phys* 2011;79:279–288.
16. American Thoracic Society. Standards for the diagnosis and care of patients with chronic obstructive pulmonary disease. *Am J Respir Crit Care Med* 1995;152:S77–S83.
17. Zaporozham J, Ley S, Eberhardt R, *et al.* Paired inspiratory/expiratory volumetric thin-slice CT scans for emphysema analysis. *Chest* 2005; 128:3212–3220.
18. Matuszak MM, Yan D, Grills I, *et al.* Clinical applications of volumetric modulated arc therapy. *Int J Radiat Oncol Biol Phys* 2010;77:608–616.
19. Schallenkamp JM, Miller RC, Brinkmann DH, *et al.* Incidence of radiation pneumonitis after thoracic irradiation: Dose-volume correlates. *Int J Radiat Oncol Biol Phys* 2007;67:410–416.

ANTICANCER RESEARCH *32*: 4533-4538 (2012)

Clinical Outcomes of Thoracic Radiotherapy for Locally Advanced NSCLC with *EGFR* Mutations or *EML4-ALK* Rearrangement

HIDETOSHI HAYASHI[1], ISAMU OKAMOTO[1], HIDEHARU KIMURA[2], KAZUKO SAKAI[2], YASUMASA NISHIMURA[3], KAZUTO NISHIO[2] and KAZUHIKO NAKAGAWA[1]

Departments of [1]Medical Oncology, [2]Genome Biology and [3]Radiation Oncology, Kinki University Faculty of Medicine, Osaka-Sayama, Osaka, Japan

Abstract. *Background: Little is known about the occurrence and consequences of epidermal growth factor receptor gene (EGFR) mutations and the fusion of the echinoderm microtubule-associated protein-like 4 (EML4) and anaplastic lymphoma kinase (ALK) genes in locally advanced non-small cell lung cancer (NSCLC). Patients and Methods: We retrospectively examined 37 patients with locally advanced NSCLC treated with definitive thoracic radiotherapy (TRT). Characteristics were compared among patients classified positive for EGFR mutations, EML4–ALK rearrangement, or patients who were double-negative for these changes. Results: We identified 11 (29.7%) patients with EGFR mutations and 3 (8.1%) with an EML4–ALK rearrangement. Progression-free survival of patients with EGFR mutation-positive NSCLC was similar to the one of those with double-negative disease (13.1 and 18.6 months). The incidence of local recurrence was higher in EGFR mutation–positive patients with NSCLC than in double-negative NSCLC. Conclusion: EGFR mutations and the EML4–ALK rearrangements were detected in substantial proportions of patients with locally advanced NSCLC. The efficacy of TRT was limited in patients with EGFR mutations.*

Lung cancer remains the most common cause of cancer-related mortality worldwide (1). Non-small cell lung cancer (NSCLC) is a heterogeneous disease that accounts for ~80% of lung cancer cases, and about one-third of individuals with newly-diagnosed NSCLC present with locally advanced disease that is not amenable to curative resection (2). The current standard of care for patients with unresectable locally advanced NSCLC is concurrent chemotherapy and definitive thoracic radiation therapy (TRT); however, most treated individuals experience disease recurrence, with the 5-year survival rate being only ~20% (3-5). Further improvement of treatment outcome for patients with locally advanced NSCLC will require the development of more effective combined-modality therapies.

The recent identification of mutations in the epidermal growth factor receptor gene (*EGFR*) in individuals with NSCLC, with these mutations occurring in 25 to 50% of Asian patients with metastatic NSCLC, has opened-up new options for the treatment of this disease (6-8). Several pivotal phase III trials have revealed that first-line treatment with EGFR tyrosine kinase inhibitors (EGFR-TKIs), rather than chemotherapy, confers a progression-free survival (PFS) and quality of life benefit in patients with metastatic NSCLC who harbor *EGFR* mutations (9-12). However, the frequency of *EGFR* mutations in individuals with locally advanced NSCLC remains unclear. It is also unclear whether patients with EGFR mutations manifest responses to TRT, including chemoradiotherapy, similar to those of patients with wild-type *EGFR*.

Even more recently, a novel fusion protein with transforming activity that is generated as a result of a chromosomal translocation involving the echinoderm microtubule-associated protein-like 4 gene (*EML4*) at chromosome 2p21 and the anaplastic lymphoma kinase gene (*ALK*) at 2p23 has been identified in a subset of NSCLC cases (13). Individuals with metastatic NSCLC who harbor the *EML4–ALK* rearrangement have shown a marked clinical response to a novel inhibitor of ALK tyrosine kinase activity. *EML4–ALK* has been detected in 4 to 5% of patients with advanced NSCLC, but little is known of the frequency of this fusion gene in individuals with locally advanced disease.

In the present retrospective study, we determined the frequency of *EGFR* mutations and the *EML4–ALK* rearrangement in a cohort of patients with locally advanced adenocarcinoma of the lung and we evaluated the clinical responses of these patients to TRT.

Correspondence to: Isamu Okamoto, Department of Medical Oncology, Kinki University Facluty of Medicine, 377-2 Ohno-higashi, Osaka-Sayama, Osaka 589-8511, Japan. Tel: +81 723660221, Fax: +81 723605000. e-mail: chi-okamoto@dotd.med.kindai.ac.jp

Key Words: Non-small cell lung cancer, radiation therapy, *EGFR* mutation, *EML4-ALK*, locally advanced lung cancer.

0250-7005/2012 $2.00+.40